The Mechanical Properties of *Drosophila* Jump Muscle Expressing Wild-Type and Embryonic Myosin Isoforms

Catherine C. Eldred,[†△] Dimitre R. Simeonov,[†△] Ryan A. Koppes,[‡] Chaoxing Yang,[†] David T. Corr,[‡] and Douglas M. Swank[†*]

[†]Department of Biology and Center for Biotechnology and Interdisciplinary Studies, and [‡]Department of Biomedical Engineering, Rensselaer Polytechnic Institute, Troy, New York

ABSTRACT Transgenic *Drosophila* are highly useful for structure-function studies of muscle proteins. However, our ability to mechanically analyze transgenically expressed mutant proteins in *Drosophila* muscles has been limited to the skinned indirect flight muscle preparation. We have developed a new muscle preparation using the *Drosophila* tergal depressor of the trochanter (TDT or jump) muscle that increases our experimental repertoire to include maximum shortening velocity (V_{slack}), force-velocity curves and steady-state power generation; experiments not possible using indirect flight muscle fibers. When transgenically expressing its wild-type myosin isoform (Tr-WT) the TDT is equivalent to a very fast vertebrate muscle. TDT has a V_{slack} equal to 6.1 $\pm$ 0.3 ML/s at 15°C, a steep tension-pCa curve, isometric tension of 37 $\pm$ 3 mN/mm^2, and maximum power production at 26% of isometric tension. Transgenically expressing an embryonic myosin isoform in the TDT muscle increased isometric tension 1.4-fold, but decreased V_{slack} 50% resulting in no significant difference in maximum power production compared to Tr-WT. *Drosophila* expressing embryonic myosin jumped <50% as far as Tr-WT that, along with comparisons to frog jump muscle studies, suggests fast muscle shortening velocity is relatively more important than high tension generation for *Drosophila* jumping.

INTRODUCTION

Myosin isoforms are major determinants of muscle contractile properties, especially maximum shortening velocity (1,2). The influence of myosin isoforms has been well studied by indirect means, such as altering expression of myosin isoforms in a muscle type through muscle activity level (3,4). Similarly, most myosin heavy chain structure-function manipulations have been evaluated in vitro (5–8) with only a few instances of direct evaluation in a working muscle (9–11), most of which have been accomplished using the *Drosophila* system (12–17).

The *Drosophila* system can be manipulated to transgenically express myosin and other muscle proteins allowing for the examination of the influence of isoform differences and protein structure directly in functioning muscle (18–20). We have previously mechanically evaluated chimeric and mutated myosins using the skinned indirect flight muscle (IFM) preparation (13–16,21). The IFM is ideal for evaluating changes in oscillatory power, stiffness, and cross-bridge rate constants. IFM functions similarly to mammalian heart muscle as its primary role is to generate oscillatory work and power, assisted by a prominent stretch activation mechanism (22–25). However, IFM fibers are limited as a tool for evaluating mechanical performance because it is not possible to measure unloaded shortening velocity and produce complete force-velocity curves due to its very short, relatively inextensible I-band (26). Another muscle in the *Drosophila* thorax, the tergal depressor of the trochanter (TDT, also known as the jump muscle, Fig. 1), is also large enough for mechanical measurements (27), and its longer, extensible I-band should enable us to expand our repertoire of measurements. Only one previous study has attempted to use the isolated TDT for mechanical analysis (27). This study measured transient step responses and tension generation using the entire TDT muscle, but did not report any measurements of shortening velocity, force-velocity, or muscle power.

The TDT, which powers jumping in the fly, structurally resembles vertebrate skeletal muscle more closely than does the IFM (27–29). The TDT is made up of ~32 fibers (27). We can transgenically replace the endogenous TDT muscle myosin isoform with other myosin isoforms or mutant myosins, as we have done with the IFM, because *Mhc*^{10} *Drosophila* mutants have no endogenous myosin in their TDT muscles (30). Wells et al. (31) showed that other myosin isoforms could be forced to replace the endogenous TDT isoform by transgenically expressing an embryonic isoform (EMB) in all muscles including the TDT. The TDT muscle was still functional as the flies could jump and myofilament ultrastructure was not adversely affected.

We have developed a TDT preparation that provides highly reproducible steady-state mechanical results when transgenically expressing either its wild-type isoform (Tr-WT) or EMB. We have made the first measurements of *Drosophila* TDT muscle shortening velocity and steady-state power generation. Expressing EMB in the TDT

Submitted January 23, 2009, and accepted for publication November 10, 2009.

△Catherine C. Eldred and Dimitre R. Simeonov contributed equally to this work.

*Correspondence: swankd@rpi.edu

Editor: Christopher Lewis Berger.

0006-3495/10/04/1218/9 $2.00

doi: 10.1016/j.bpj.2009.11.051

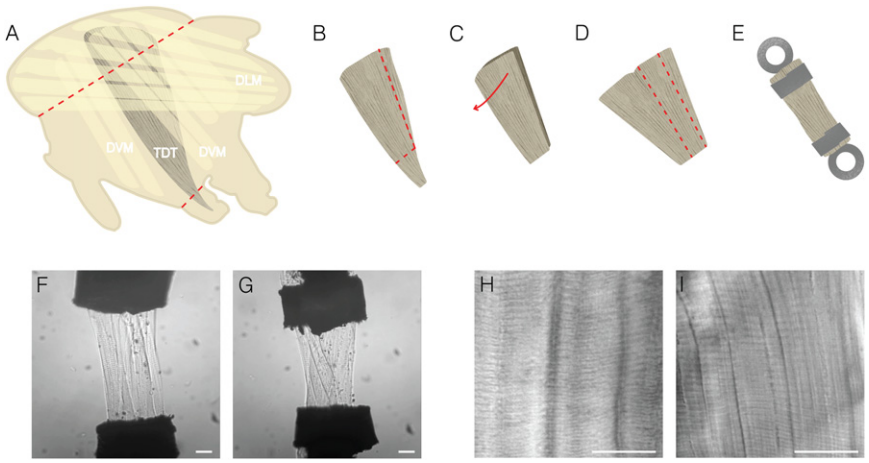

FIGURE 1 (*A*) Anatomy and location of the TDT muscle. The TDT is represented in dark gray for visibility among the other major muscles of the *Drosophila* thorax, the DLM (horizontal IFM fibers, *yellow*) and DVM (vertical IFM fibers, *yellow*). The TDT is translucent and difficult to observe during dissection. The red dotted lines mark the location of the two cuts through a half thorax that are made to free the TDT from the thoracic cuticle. (*B*) The free TDT is cut just above the end of the tendon and down the side to remove the four smaller diameter fibers. (*C*) The TDT is composed of two fiber layers so that the vertical cut allows it to open up into one layer with a thickness of a single fiber. (*D*) The TDT is split parallel to the fibers producing a preparation consisting of 8–10 fibers. (*E*) Each end of the TDT is clipped in laser cut T-clips, which is then mounted on the muscle mechanics rig using hooks extending from the force transducer and servo motor. (*F*) A Tr-WT TDT preparation mounted on the mechanics rig, in relaxing solution, showing good alignment of fibers between the T-clips. This preparation produced excellent force-velocity data. (*G*) An EMB preparation that produced poor quality data as the fibers were twisted while T-clipping the preparation. Both Tr-WT and EMB TDT muscle fiber bundles produce equally good data if the preparations are as good as the one in *F*. (*H*) A differential interference contrast image of a Tr-WT TDT muscle that was dissected from a 2-day old fly and imaged in Ringer's solution without staining or fixation. (*I*) Same as *F*, except this TDT expresses EMB. Both EMB and control fibers display normal sarcomere patterns. Scale bars = 30 μm.

decreases the force-pCa Hill coefficient, increases isometric tension, decreases maximum velocity of shortening (V_{slack}), but does not significantly decrease maximum power production during constant shortening. Overall, these results show the high value of our TDT preparation for mechanically analyzing the functional consequences of mutated myosin and other muscle proteins transgenically expressed in *Drosophila*.

METHODS

Transgenic *Drosophila* lines

Creation of the *pwMhc2 Drosophila* transgenic line (Tr-WT) is described in Swank et al. (5). This line contains a transgenic copy of the *Mhc* gene with flanking 5′ and 3′ regions, including the *Mhc* promoter. The transgene expresses the specific native myosin isoform normally found in each muscle fiber type. When crossed with the *Drosophila* line Mhc^{10}, null for myosin expression in the IFM and TDT muscles (30), only the transgenic TDT myosin isoforms is expressed in the TDT. This line displayed normal jumping ability and ultrastructure (32). Creation of the EMB transgenic line is described in Wells et al. (31). This line uses a cDNA construct encoding an embryonic isoform behind the myosin promoter to express an embryonic cDNA in all *Drosophila* muscles. Crossed with Mhc^{10}, the TDT only expresses the EMB myosin isoform.

TDT muscle preparation

TDT muscle fibers were dissected from the thoraces of 2–3-day-old female *Drosophila* (Fig. 1) and chemically demembranated (skinned) in dissection solution (5 mM MgATP, 1 mM free Mg^{2+}, 5 mM EGTA, 20 mM BES (pH 7.0), 175 mM ionic strength, adjusted with Na methane sulfonate, 1 mM DTT, 0.5% Triton X-100 and 50% glycerol) for 1 h at 4°C.

The TDT preparation, consisting of 8–10 large diameter fibers, was mounted on the fiber mechanics rig using T-clips laser cut from food grade aluminum foil (MicroConnex, Snoqualmie, WA) (Fig. 1, *E–G*). The hole in the base end of the T-clip was sized so that it fit snugly over the mounting hooks that extend from the force transducer and servo motor to minimize movement of the T-clip on the wire during length perturbations. The resulting dimensions of the preparation, between the proximal ends of the clips, averaged ~125 μm in length, 110 μm in width, and 45 μm in depth.

The mechanics rig used for the slack-test experiments was similar to the IFM rig described previously (13) with the following modifications. A rectangular prism was adhered to the glass bottom of the chamber to allow, in addition to the length and width, the height of the muscle fiber to be measured using a compound microscope and video analysis software (Ion Optix, Milton, MA). The same software package was used to obtain average TDT sarcomere length. A video image of the TDT muscle was captured from an inverted compound microscope with a 40× objective. Measurements from three different fibers in the muscle bundle (top, middle, and bottom) were averaged to determine sarcomere length. The servo motor was a P-841.20 (Physik Instrumente, Karlsruhe, Germany) with a 30 μm throw and $<$ 0.5 ms response time when used with position feedback. Changes in the ionic composition of the muscle bathing solution were accomplished by partial solution exchanges in one chamber. The mechanics rig was controlled by custom written software (33).

Mechanical protocol for measuring TDT unloaded shortening velocity

TDT muscle fiber bundles were mounted in relaxing solution (260 mM ionic strength, adjusted with Na methane sulfonate, 10 mM MgATP, 45 mM creatine phosphate, 1200 U/mL creatine phosphokinase, 1 mM free Mg^{2+}, 5 mM EGTA, 20 mM BES (pH 7.0), and 1 mM DTT) at 15°C. The fibers were stretched until they reached an average sarcomere length of 3.6 μm (Fig. 1, *F* and *G*). A preactivating solution (same as relaxing solution but with lower, 0.5 mM, EGTA) was exchanged into the bathing solution chamber to help ensure sarcomere homogeneity during activation (34). The fiber was activated to pCa 5.0 by three partial solution exchanges of the preactivating solution with activating solution (same as relaxing solution, but with calcium content adjusted to pCa 4.0). The slack test was used to measure shortening velocity (V_{slack}) (33,35) by very rapidly shortening a fully active muscle in <5 ms. This reduced force levels to zero; the muscle is slack. The time taken for the force level to rise above zero, when slack is eliminated from the muscle, was measured. The maximum unloaded muscle shortening speed was determined by plotting multiple muscle length changes versus time required to take up slack. Isometric tension was measured immediately before and after each slack test.

Mechanical set-up for tension-length, tension-pCa, and tension-velocity measurements

To improve the longevity of the fiber preparation, we used a multiple-well rig for the tension-length, tension-velocity, and tension-pCa measurements. This rig is similar to the one used for the slack-tests, but has 14 solution wells between which the fiber can be quickly transferred. This allowed for rapid relaxation of the fiber between shortening steps.

Tension-length curve protocol

To establish the appropriate starting sarcomere length so that the slack-tests and force-clamps were carried out over sarcomere lengths where maximum or nearly maximum tension is generated, the Tr-WT and EMB tension-length profile was determined. Resting tension was measured in relaxing solution. The fiber was transferred to preactivating solution, where sarcomere length was set, then transferred to activating solution, pCa 5.0, where tension was measured, and returned to relaxing solution. To control for fatigue effects, for half of the fibers sarcomere length was initially set at 4.0 μm and shortened by 0.1 μm increments to 3.0 μm. For the other half of the fiber set, sarcomere length was initially set at 3.0 μm and lengthened to 4.0 μm by 0.1 μm increments.

Tension-pCa protocol

Muscle fibers, at a sarcomere length of 3.6 μm, were sequentially transferred into higher or lower calcium concentration solutions and isometric tension was measured at each concentration. Between each calcium concentration, the muscle was returned to relaxing solution and transferred into preactivating solution. For half of the fibers, the order of calcium solutions was reversed.

Tension-velocity protocol

To determine TDT shortening velocity at different loads and steady-state power generation, we used the force-clamp technique (33,36). Fibers were activated after preactivation solution and rapidly shortened until the tension level dropped to a predetermined set level. Reaching the set level required less than 8 ms for the greatest drop in tension. Tension levels were monitored by feeding back the output of the force gauge to the servo motor system. Velocity was measured over an average time period of 8 ms once force was clamped. This time period required the muscle to shorten at most by 12% for the lowest forces clamped. Percent maximum tension clamped was plotted versus velocity, and tension multiplied by velocity to determine power. The fiber was relaxed between each force-clamp shortening run.

Jump testing

Jump ability was the horizontal distance a *Drosophila* could jump off a 10-cm high platform at 22°C. The flies' wings were removed before jump testing. The average distance of the three longest jumps out of 10 trials per fly was reported. Flies were 2–4-day-old females.

RESULTS

Jumping ability

Drosophila expressing EMB myosin in their TDT muscle jumped only 40% as far as Tr-WT flies, but were able to jump 1.5-fold farther than *Drosophila* with no myosin in their TDT muscles, Mhc^{10} (Table 1). Minor leg muscles, that express a different myosin isoform than the TDT, accounted for some jumping ability, or at least the ability to walk off the edge of the platform, by Mhc^{10} *Drosophila*.

TABLE 1 ***Drosophila*** **jump performance**

Fly line	Jump distance (cm)
Tr-WT	5.6 ± 0.2*
EMB, 34	2.4 ± 0.1*
EMB, 44	2.4 ± 0.1*
EMB, 38	2.2 ± 0.1*
Mhc^{10}	1.6 ± 0.1

EMB, embryonic isoform; Tr-WT, wild-type myosin isoform.
*Statistically different from Mhc^{10} ($p < 0.05$, t-test). The three EMB lines were created by independent insertion events. We only used EMB, 34 for all the mechanics experiments as we have previously shown that this line expresses myosin at normal levels in the IFM, and that IFM mechanical measurements on EMB, 34 and 44 produce the same values (15). Similarly, the Tr-WT fly line expresses myosin at wild-type levels and equivalent IFM mechanical results have been obtained with another Tr-WT line (15). $n = 40$ flies for each line.

TDT muscle mechanics

To measure power and other mechanical properties, we made several improvements in the TDT preparation that resulted in a more robust and reliable preparation compared to the preparation used in the only previous TDT mechanical study (27). Our preparation enables additional types of mechanical measurements, such as shortening velocity and steady-state power generation. We pared down the muscle to a small bundle of 8–10 fibers rather than using the entire muscle. This resulted in faster activation and less damage to the muscle as it was more securely and uniformly held in the T-clips. The TDT activated faster and was less likely to rip when a preactivating solution (0.5 mM EGTA, pCa 8.0) was interposed between relaxing and activating solutions rather than transferring the muscle directly from a relaxing solution at pCa 8.0 (5 mM EGTA) to an activating solution at pCa 5.0. This improvement was likely due to faster and more uniform calcium entry and binding to troponin C in each sarcomere (34). Aligning TDT fibers as parallel as possible to each other and in the direction of shortening (Fig. 1, *F* and *G*) produced better quality slack-test and force-clamp data.

We compared exchanging bathing solutions around the TDT in a single chamber muscle mechanics rig to moving the TDT into different chambers in a multi-well rig to determine which set-up produced better quality data and less fiber fatigue. In a single chamber rig, a fully activated TDT muscle fiber could be subjected to about six different solution conditions, with three slack test measurements under each condition, before excessive muscle fatigue. If the muscle was relaxed after each run by using a multi-well rig, then the TDT muscle lasted at least twice as long and there was less loss of force producing ability.

Isometric tension

Relaxed tension of TDT muscle expressing either Tr-WT or EMB myosin was very low, especially compared to the other major thoracic muscle in the fly, IFM (Table 2). This was

TABLE 2 Mechanical properties of TDT muscle expressing Tr-WT and EMB myosin isoforms

	Resting tension	T_{max}	pCa_{50}	Hill coefficient	V_{slack}
Tr-WT	0.9 ± 0.2 (mN/mm^2)	37 ± 3 (mN/mm^2)	5.62 ± 0.01	10.2 ± 2.1	6.1 ± 0.3 (ML/s)
EMB	2.1 ± 0.5	53 ± 5*	5.67 ± 0.02*	6.3 ± 0.9*	3.1 ± 0.2*

EMB, embryonic isoform; ML, muscle length; T_{max}, maximum calcium activated tension; Tr-WT, wild-type myosin isoform; V_{slack}, velocity determined using the slack test.

Tension values were measured at a SL = 3.6 μm. pCa_{50} and the Hill coefficient were determined by fitting the tension-pCa response with the Hill equation (Fig. 2). Values are mean ± SE.

*Significantly different from Tr-WT, $p < 0.05$, Student's *t*-test. $n = 7$ and 8 for Tr-WT and EMB resting tension, respectively. $n = 21$ and 23 for Tr-WT and EMB active tension, respectively. $n = 6$ for pCa 50 and Hill coefficient, $n = 10$ for V_{slack}.

particularly apparent when the ratios of passive to active tension for the two muscle types were compared. For TDT, net active tension was ~30-fold higher than passive tension for both isoforms, whereas all myosins tested in the IFM had passive tension levels almost equal to net active tension (Table 2) (14–16,21).

To determine if passive tension increases significantly with increasing sarcomere length, we measured tension over a sarcomere range of 3.0–4.0 μm. At sarcomere lengths of 3.0 and 4.0 μm, we measured passive tension values of 0.5 ± 0.15 mN/mm^2 and 3.1 ± 0.8 mN/mm^2 respectively, for TDT expressing EMB, and 1.0 ± 0.2 mN/mm^2 and 1.2 ± 0.3 mN/mm^2, respectively, for TDT expressing Tr-WT. The EMB relaxed tension values were significantly different ($p = 0.005$, Student's *t*-test, $n = 8$), whereas for Tr-WT, the values were not significantly different at these two sarcomere lengths ($p = 0.6$; $n = 7$).

Active tension of Tr-WT TDT muscle was 37 ± 3 mN/mm^2 at phosphate (Pi) and MgATP concentrations of 0 mM and 20 mM, respectively, at a sarcomere length of 3.6 μm (Table 2). Expressing EMB myosin increased tension 1.4-fold, under these conditions, compared to control TDT (Fig. 2, *inset*).

We tested the TDT tension profile with changing sarcomere length to determine if, during the slack test and force-clamp experiments, the degree of sarcomere shortening would lead to appreciable declines in TDT tension generating ability. At sarcomere lengths of 3.0 and 4.0 μm, we measured net active tension values of 41 ± 16 mN/mm^2 and 45 ± 18 mN/mm^2, respectively, for TDT expressing EMB, and 25 ± 4 mN/mm^2 and 29 ± 4 mN/mm^2 for TDT expressing Tr-WT. For both EMB and Tr-WT, the active tension values were not significantly different ($p \geq 0.05$, Student's *t*-test, $n = 4$ for EMB and $n = 7$ for Tr-WT) at these two sarcomere lengths. Comparing our data to tension-length curves of frog semimembranosus single fibers (37) suggests that we are operating on the shallow ascending limb, plateau and perhaps slightly down the descending limb of the tension-length curve. Over this sarcomere range (1.6–2.6 μm, the same 1 μm distance as in our study) tension would only be expected to decrease by 10–12% from maximum tension. Our tension results are within this range. Our slack tests shortened the TDT a maximum of 15% that, with a starting sarcomere length of 3.6 μm, results in the muscle bundle shortening to 3.05 μm.

Tension response to calcium

TDT expressing Tr-WT displayed a very steep tension-pCa curve, which we determined by incrementally increasing calcium concentration from pCa 8 to 5.0 (Fig. 2). The Hill coefficient was 10.2 ± 2.1 with a pCa_{50} of 5.62 ± 0.01 (Table 2). The shape of the curve was altered by the expression of EMB in TDT. EMB produced higher force levels at lower calcium concentrations, as seen in an increased pCa_{50} and decreased Hill coefficient (Table 2 and Fig. 2).

Unloaded shortening velocity

Both Tr-WT and EMB TDT fibers produced very good slack-test traces (Fig. 3). The start of force regeneration is clearly demarcated that is critical for accurate maximum velocity calculations. The velocity of TDT expressing Tr-WT was 6.1 ± 0.3 ML/s at a starting sarcomere length of 3.6 μm

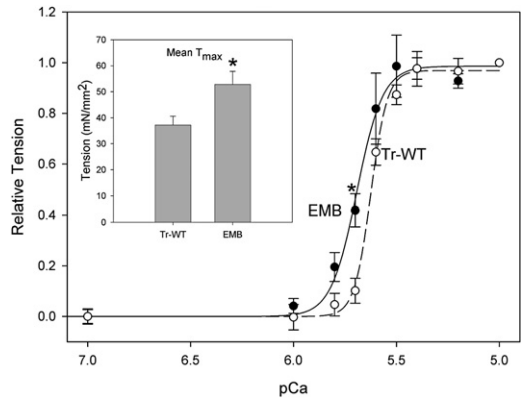

FIGURE 2 Isometric tension-pCa relationships. Tension generated by TDT fibers was measured at a sarcomere length of 3.6 μm. Tension was normalized to equal 1 at pCa 5.0 and fit with a standard Hill curve. There is a significant leftward shift of the bottom of the curve when expressing EMB myosin as seen by the significant tension difference at pCa 5.7 ($p < 0.05$, *t*-test) and significant differences in the Hill coefficient and pCa_{50} values (Table 2). $n = 6$ for each fiber type. *Inset*: Isometric tension of EMB TDT muscle, at saturating calcium, pCa 5.0, was significantly higher than Tr-WT TDT fibers ($p < 0.05$, *t*-test). $n = 21$ for Tr-WT and $n = 23$ for EMB. All values are mean ± SE.

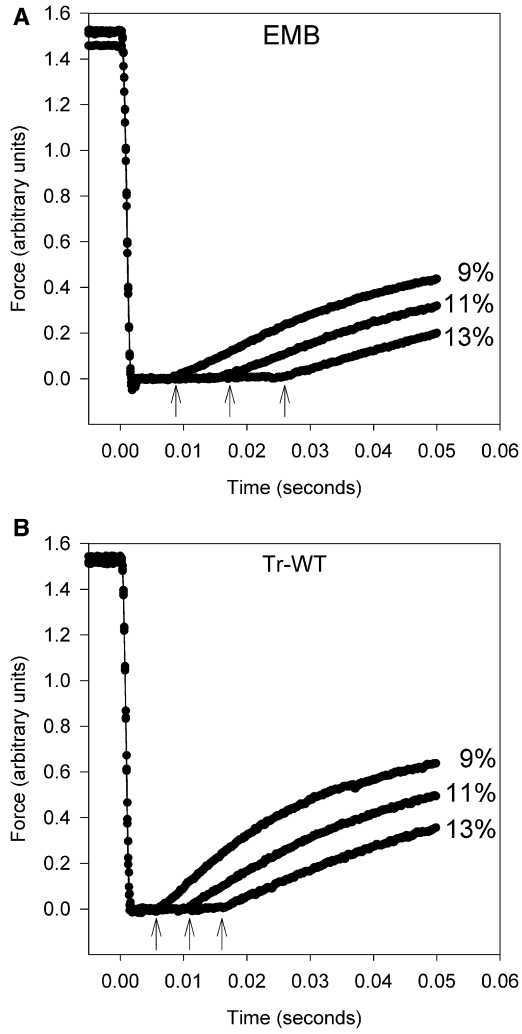

FIGURE 3 Unloaded shortening velocity (V_{slack}) was measured using the slack test. (*A*) Raw data from TDT muscle expressing EMB showing the time to force redevelopment for three different shortening amounts, expressed as percent of muscle length. Arrows indicate the points at which force redevelopment starts. (*B*) Slack test data from Tr-WT TDT fibers showing the earlier time points at which force redevelopment starts compared to EMB. The slope of percent length change against time was determined to calculate the shortening velocities shown in Table 2. Time 0 equals the start of shortening.

and a solution composition of 0 mM Pi and 20 mM MgATP. TDT muscle expressing Tr-WT shortens almost 2-fold faster than TDT muscle expressing EMB under these conditions (Table 2).

Velocity under load

We believe our new TDT preparation was highly useful for measuring shortening velocity at different loads and steady-state power generation (Fig. 4). We were able to clamp forces within 8 ms of the start of shortening (Fig. 4, *A* and *B*). Plotting the velocity values for each clamped force value revealed that the shortening velocity of Tr-WT TDT was greater than EMB TDT shortening velocity below tension levels of ~20% of maximum (Fig. 4 *C*). Fitting the data with the hyperbolic Hill curve (33), and no difference in a/T_{max} (Table 3) showed that the shapes of the force-velocity curves were similar. Extrapolating the tension-velocity curves to zero tension showed that EMB V_{max} was 63% of Tr-WT (Table 3). The maximum shortening values (V_{max}) were very similar to those determined by the slack-test (V_{slack}) as Tr-WT V_{slack} was only 16% lower than Tr-WT V_{max} and the EMB values were not statistically different (Tables 2 and 3). The force levels that produced maximum power were ~25% of T_{max} for both Tr-WT and TDT. Due to the high degree of curvature to the tension-velocity plot, the velocity that produced maximum power generation was also ~25% of V_{max} for both Tr-WT and EMB TDT muscles (Table 3). When tension is normalized, Tr-WT power appears higher than EMB power when plotted versus velocity (Fig. 4 *D*). However, taking into account the difference in maximum isometric tension (T_{max}, Table 2), the maximum steady-state power generated by Tr-WT and EMB are not significantly different (Table 3, *column 7*).

DISCUSSION

We have shown that the TDT muscle preparation, when combined with the genetic advantages of *Drosophila*, is a valuable tool for examining muscle protein structure/function relations. We can run a full complement of mechanical measurements on the TDT preparation including maximum shortening velocity (V_{slack}), shortening velocity under different loads and steady-state power production. Although *Drosophila* IFM has been used extensively for mechanical measurements, such as oscillatory power production (16,21), its very short, inextensible I-band limits the distance its sarcomeres can lengthen or shorten (26); hence, it is not suitable for V_{slack} and force-velocity measurements that require >10% shortening of sarcomeres. In contrast, the TDT is a particularly good preparation for slack-test and force-velocity experiments as its I-bands are highly extensible with long thick and thin filaments (26). Thus, the required shortening during experiments can occur without a significant decrease in force production. TDT active tension generation is high and relaxed tension very low, the opposite of IFM. This makes some mechanical measurements, such as force-pCa curves, easier and more accurate with TDT muscle.

Our dissection and handling of the TDT differed considerably from the sole previous study in which the TDT was mechanically evaluated (27). This study used the entire muscle, T-clipping the tendon that inserts into the middle leg, and the dorsal end of the muscle that was left attached to its insertion with the thoracic cuticle (John Sparrow, University of York, personal communication, 2004). Using a whole muscle probably limited the effectiveness and types of experiments that could be carried out, as we often observed slow or no activation when using an entire TDT muscle. When the whole TDT did activate, the fibers were

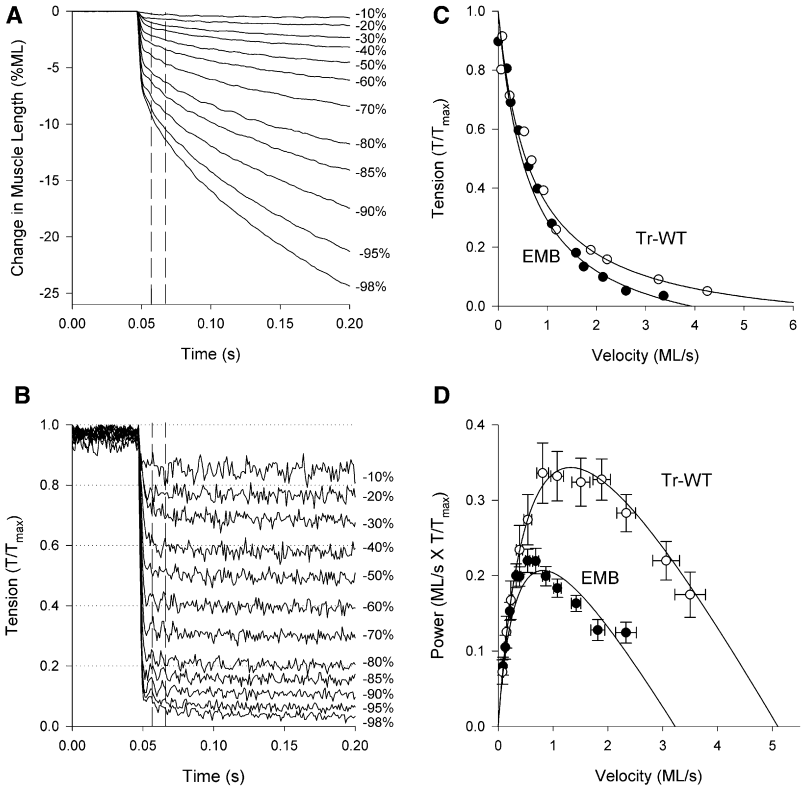

FIGURE 4 TDT tension-velocity and power measured using the force-clamp technique. (*A*) Raw position traces from a Tr-WT TDT showing the percent ML slope required to achieve the tension level written at the end of the trace. Tension values are percent of maximum isometric tension. Vertical dashed lines show the approximate range over which shortening velocity was measured. (*B*) The corresponding tension traces from the same muscle preparation. (*C*) Velocities, calculated from the slope of the traces in *A*, were plotted against tension that was normalized to equal 1 at maximum isometric tension. The Tr-WT curve was generated from the data shown in *A* and *B*, whereas the EMB curve is from raw data not shown. Both curves were fit with the Hill curve. (*D*) Mechanical power calculated from multiplying average tension and velocity values, and fit with curves generated from multiplying the tension and velocity from the average Hill curves. Although the maximum power generated by Tr-WT is higher than EMB when tension is normalized, maximum power generation is not significantly different between the fiber types when actual tension values in units of mN/mm^2 are used in the power calculation (Table 3).

likely to rip out of the T-clip. These problems were probably due to inhomogeneous calcium diffusion into the whole muscle and the difficulties of securely attaching and aligning all the fibers in parallel between the T-clips. To counter these challenges, we prepared a shorter and thinner preparation, taken from a region of the TDT where the fibers are parallel to each other (Fig. 1). We used a preactivating solution to ensure uniform calcium entry, and a creatine phosphate MgATP regeneration system to buffer MgATP concentrations and to keep MgADP near 0 mM. With these improvements, we could carry out a wider range of mechanical measurements on the TDT muscle.

New *Drosophila* muscle mechanical measurements using the TDT

We made the first maximum shortening velocity measurements of the TDT muscle. The TDT muscle is a very fast muscle type as its V_{slack} was 6.1 ML/s at 15°C (Table 2). This is comparable to mouse fast 2X and 2B skeletal muscle, 4.3 and 6.5 ML/s at 12°C (38), and thus faster than all mammals larger than a mouse as muscle velocity decreases with increasing body mass (39). The TDT is slower than rattlesnake shaker muscle and toadfish swim bladder, 7.6 and 11.8 ML/s at 16°C respectively, two of the fastest known vertebrate muscle types (40,41). However, these muscles are designed for oscillatory speed. TDT shortening speed is similar or faster than two of the fastest vertebrate muscles that have evolved for rapid shortening to power jumping, the anterior tibialis, 4.1 ML/s at 7.5°C and semimembranosus, 10.4 ML/s at 25°C from *Rana pipiens* (37,42).

Power for jumping

The fast shortening velocity, higher active tension generation, lower passive tension, extensible I-bands, and other

TABLE 3 *Drosophila* TDT muscle fiber mechanics as measured by force-clamp analysis

	a/T_{max} (no units)	b (ML/s)	V_{max} (ML/s)	V_{opt} (ML/s)	T_{opt}/T_{max} (%)	p_{max} (ML/s × T/T_{max})	p_{max} (ML/s × mN/mm^2)
Tr-WT	0.15 ± 0.02	0.77 ± 0.10	5.10 ± 0.34	1.34 ± 0.08	26 ± 1	0.35 ± 0.03	12.9 ± 1.4
EMB	0.14 ± 0.03	0.43 ± 0.04*	3.23 ± 0.38*	0.85 ± 0.06*	25 ± 1*	0.20 ± 0.01*	11.3 ± 1.4

a, fitted parameter based on Hill's equation; b, fitted parameter based on Hill's equation; ML, muscle length; p_{max}, maximum power; T_{max}, maximum activated tension; T_{opt}, tension at maximum power; Tr-WT, wild-type myosin isoform; V_{max}, maximum shortening velocity extrapolated from the Hill fit of tension-velocity curves; V_{opt}, velocity at maximum power.

The p_{max} values in the final column were calculated using V_{opt}, T_{opt}/T_{max}, and T_{max} from Table 2. $n = 10$ for both Tr-WT and EMB. Values are mean ± SE.
*Significantly different from Tr-WT, $p < 0.05$, Student's *t*-test.

differences of TDT compared to IFM reflect the different evolutionary constraints of the TDT. Responsible for the extension of the mesothoracic legs, the TDT muscle acts as the main contributor to jumping force and power production during two types of take-offs that initiate flight (28,29,43). We compared TDT mechanical power generation to a rough estimate of the average power required for jumping. Zumstein et al. (29) inferred an average power generation of 1.5 W g^{-1} in TDT muscle during the 5 ms take-off period, based on estimated TDT mass, measured jump distances and the kinetic energy required to propel wingless *Drosophila*. Using our average preparation length (125 μm), cross section area (4950 μm^2), and data from our force-clamp experiments (Fig. 4 and Table 3), we calculated a maximum power generation of 8.06 nW and 6.95 nW for TDT expressing Tr-WT and EMB, respectively. Incorporating a muscle density of 1.0×10^{-6} $\mu g/\mu m^3$ (29), and our average muscle preparation dimensions, results in a maximum specific power of 13.0 mW g^{-1} and 11.2 mW g^{-1} for TDT expressing Tr-WT and EMB, respectively. This falls well below the results of Zumstein's in vivo analysis (29). This discrepancy in power production can be attributed to the different methods used to calculate power. Whereas, our calculations determine specific power directly as the instantaneous product of force and shortening velocity in a fiber bundle preparation, Zumestein et al. (29) infer TDT power generation based on energy estimates from a whole body jump. All of the energy required for the observed jump is attributed to work generated solely by the TDT muscles without consideration of muscle architecture, elastic contributions, or fiber orientation. Perhaps the most significant reason for their overprediction of muscle specific power is not incorporating the mechanical advantage of the femoral-tibial articulation of the leg, which increases the jump force the leg exerts on the ground compared to force produced by the muscle. In locusts this mechanical advantage can range from 250:1 at 0° to 17:1 at 135° of femoral extension (44). Incorporation of these anatomical factors would greatly reduce the force attributed to the TDT, thereby greatly decreasing the estimated power necessary for the observed jump.

Although lower than that predicted by Zumstein et al. (29), when compared to the performance of similar skinned fiber preparations, the power generation by *Drosophila* TDT is higher than that of most mammals. Type I skeletal muscle fibers from both the soleus and gastrocnemius of Sprague-Dawley rats, rhesus monkeys, and humans produced 4.1, 2.3, and 1.5 kN $m^{-2} \times$ ML s^{-1}, respectively at 15°C (45). Tr-WT and EMB *Drosophila* TDT skinned fiber bundles produced 12.9 kN $m^{-2} \times$ ML s^{-1} and 11.3 kN $m^{-2} \times$ ML s^{-1}, respectively (Table 3). TDT muscle produces less power than slow and fast fibers from *Xenopus* laevis, 15 mW/g and 73 mW/g, measured at 5°C (46), and much less power than the fastest fiber type found in the anterior tibialis muscle of *Rana pipiens*, 575 mW/g, measured from live single fibers at 25°C (47). Most of the power difference is due to lower force generation by the TDT as frog jumping muscles produce 5- to 7-fold more tension (37,47), suggesting that high velocity is relatively more important than high tension for *Drosophila* jumping. Our finding that the slower EMB isoform decreases jumping distance by more than half, but does not decrease TDT maximum muscle power generation also supports the greater relative importance of shortening velocity.

Expression of EMB alters mechanical performance

Our successful measurements of TDT mechanical properties when expressing EMB showed that the TDT will be very useful for mechanical evaluation of various myosin isoforms and mutants. EMB TDT mechanical data quality were equal to Tr-WT data with the same amount of error (Tables 2 and 3).

Expressing EMB transformed the TDT's tension-pCa curve to be more like a slower muscle as it was less steep, with the bottom portion shifted to the left relative to Tr-WT's curve (Fig. 2). We think the two alternative *Drosophila* myosin S-2 hinge versions (30) are responsible for the shift. The EMB hinge has been shown to be ~5 nm longer than the adult version (expressed in TDT) of the hinge due to its greater propensity to form a more rigid coiled-coil structure (48,49). Changes in length or stiffness of the hinge could influence the probability of myosin binding to the actin filament by influencing head mobility or orientation with respect to the thin filament. Alternatively, thin filament protein isoforms could be up or down regulated in response to EMB expression. Another possibility is that minor deviations in the spacing of thick and thin filaments seen when EMB is expressed in TDT (31) could be influencing the probability of myosin binding to actin.

Expressing EMB decreased TDT V_{slack} to 3.1 ML/s. This translates to the thick and thin filaments in each half-sarcomere sliding past each other at 5.6 μm/s at 15°C. If we use a conservative Q_{10} estimate of 2, this translates to 9.5 μm/s at 22°C. Thus, even when not in its native muscle type, EMB myosin kinetics are increased 13-fold compared to when EMB is propelling bare actin in the in vitro motility assay, 0.7 μm/s at 22°C, and 2.4-fold compared to when EMB is propelling actin decorated with tropomyosin, 4 μm/s at 22°C (50). Thus the actin velocity value with tropomyosin is closer to what we observed in the skinned muscle preparation. The unloaded shortening velocity of TDT expressing EMB suggests EMB may actually be a fast muscle myosin, rather than a slow muscle myosin as we have characterized it previously based on our motility assay results. Unfortunately, the embryonic and larval body wall muscles that naturally express EMB are too small for mechanical measurements so we cannot compare our results with the shortening speed of EMB in its native muscle types.

EMB produces >10-fold higher calcium activated tension in the TDT compared to when it is expressed in the IFM (16). This difference could be due to different thin filament proteins changing duty ratio, up- or downregulation of sarcomeric proteins in response to EMB expression, recruitment of a different number of myosin cross-bridges due to differences in myosin binding sites on actin between muscle fibers (51), thick and thin filament number as a percent of fiber cross-sectional, or that force generation in IFM is much higher after a quick stretch (52). We will be better able to determine the reason for tension differences once we test more myosin isoforms in both TDT and IFM, and also perform a detailed ultrastructure comparison between IFM and TDT muscle fibers.

Combining the power of *Drosophila* genetics with steady-state mechanical analysis, our new TDT preparation and oscillatory mechanical measurements using IFM, we can now carry out a comprehensive suite of mechanical perturbations to fully evaluate any transgenic muscle protein isoform or mutant. This array of techniques will allow us to answer many interesting questions such as identifying myosin structural regions critical for setting muscle shortening velocity (53).

We thank Dr. D. Maughan for loaning us the multiple well mechanics rig used for preliminary force-velocity experiments. We acknowledge W. Brown for making the first attempts at TDT dissection and the use of whole muscles for mechanical experiments. We thank S. Lee and the RPI Microscopy Core for creating the images in Figure 1. We thank Dr. B. Palmer, Department of Molecular Physiology and Biophysics at the University of Vermont, for the length perturbation acquisition software.

Financial support to D.M.S. was provided by National Institutes of Health (AR055611), American Heart Association Scientist Development (0635058N), and the Muscular Dystrophy Association (MDA68954).

REFERENCES

1. Lowey, S., G. S. Waller, and K. M. Trybus. 1993. Function of skeletal muscle myosin heavy and light chain isoforms by an in vitro motility assay. *J. Biol. Chem.* 268:20414–20418.
2. Harridge, S. D. 2007. Plasticity of human skeletal muscle: gene expression to in vivo function. *Exp. Physiol.* 92:783–797.
3. Larsson, L., X. Li, and W. R. Frontera. 1997. Effects of aging on shortening velocity and myosin isoform composition in single human skeletal muscle cells. *Am. J. Physiol.* 272:C638–C649.
4. Baldwin, K. M., and F. Haddad. 2001. Effects of different activity and inactivity paradigms on myosin heavy chain gene expression in striated muscle. *J. Appl. Physiol.* 90:345–357.
5. Swank, D. M., L. Wells, …, S. I. Bernstein. 2000. Determining structure/function relationships for Sarcomeric myosin heavy chain by genetic and transgenic manipulation of *Drosophila*. *Microsc. Res. Tech.* 50:430–442.
6. Murphy, C. T., and J. A. Spudich. 2000. Variable surface loops and myosin activity: accessories to a motor. *J. Muscle Res. Cell Motil.* 21:139–151.
7. Krenz, M., A. Sanbe, …, J. Robbins. 2003. Analysis of myosin heavy chain functionality in the heart. *J. Biol. Chem.* 278:17466–17474.
8. Rovner, A. S., Y. Freyzon, and K. M. Trybus. 1997. An insert in the motor domain determines the functional properties of expressed smooth muscle myosin isoforms. *J. Muscle Res. Cell Motil.* 18:103–110.
9. Babu, G. J., E. Loukianov, …, M. Periasamy. 2001. Loss of SM-B myosin affects muscle shortening velocity and maximal force development. *Nat. Cell Biol.* 3:1025–1029.
10. Krenz, M., S. Sadayappan, …, J. Robbins. 2007. Distribution and structure-function relationship of myosin heavy chain isoforms in the adult mouse heart. *J. Biol. Chem.* 282:24057–24064.
11. Herron, T. J., E. J. Devaney, and J. M. Metzger. 2008. Modulation of cardiac performance by motor protein gene transfer. *Ann. N. Y. Acad. Sci.* 1123:96–104.
12. Dickinson, M. H., C. J. Hyatt, …, D. W. Maughan. 1997. Phosphorylation-dependent power output of transgenic flies: an integrated study. *Biophys. J.* 73:3122–3134.
13. Yang, C., S. Ramanath, …, D. M. Swank. 2008. Alternative versions of the myosin relay domain differentially respond to load to influence *Drosophila* muscle kinetics. *Biophys. J.* 95:5228–5237.
14. Swank, D. M., J. Braddock, …, D. W. Maughan. 2006. An alternative domain near the ATP binding pocket of *Drosophila* myosin affects muscle fiber kinetics. *Biophys. J.* 90:2427–2435.
15. Swank, D. M., W. A. Kronert, …, D. W. Maughan. 2004. Alternative N-terminal regions of *Drosophila* myosin heavy chain tune muscle kinetics for optimal power output. *Biophys. J.* 87:1805–1814.
16. Swank, D. M., A. F. Knowles, …, S. I. Bernstein. 2002. The myosin converter domain modulates muscle performance. *Nat. Cell Biol.* 4:312–316.
17. Moore, J. R., M. H. Dickinson, …, D. W. Maughan. 2000. The effect of removing the N-terminal extension of the *Drosophila* myosin regulatory light chain upon flight ability and the contractile dynamics of indirect flight muscle. *Biophys. J.* 78:1431–1440.
18. Maughan, D. W., and J. O. Vigoreaux. 1999. An integrated view of insect flight muscle: genes, motor molecules, and motion. *News Physiol. Sci.* 14:87–92.
19. Cripps, R. M., and S. I. Bernstein. 2000. Generation of transgenic *Drosophila melanogaster* by *P* element-mediated germline transformation. *In* Introducing DNA into Living Cells and Organisms. P. A. Norton and L. F. Steel, editors. Bio Techniques Books, Eaton Publishing, Natick, MA.
20. Sparrow, J., D. Drummond, …, D. White. 1991. Protein engineering and the study of muscle contraction in *Drosophila* flight muscles. *J. Cell Sci. Suppl.* 14:73–78.
21. Swank, D. M., V. K. Vishnudas, and D. W. Maughan. 2006. An exceptionally fast actomyosin reaction powers insect flight muscle. *Proc. Natl. Acad. Sci. USA.* 103:17543–17547.
22. Steiger, G. J. 1977. Stretch activation and tension transients in cardiac, skeletal and insect flight muscle. *In* Insect Flight Muscle. R. T. Tregear, editor. North Holland, Amsterdam, pp. 221–268.
23. Moss, R. L., and D. P. Fitzsimons. 2002. Frank-Starling relationship: long on importance, short on mechanism. *Circ. Res.* 90:11–13.
24. Steiger, G. J. 1971. Stretch activation and myogenic oscillation of isolated contractile structures of heart muscle. *Pflugers Arch.* 330:347–361.
25. Pringle, J. W. S. 1978. The Croonian Lecture, 1977. Stretch activation of muscle: function and mechanism. *Proc R Soc Lond B Biol Sci.* 201:107–130.
26. Burkart, C., F. Qiu, …, B. Bullard. 2007. Modular proteins from the *Drosophila sallimus* (*sls*) gene and their expression in muscles with different extensibility. *J. Mol. Biol.* 367:953–969.
27. Peckham, M., J. E. Molloy, …, D. C. White. 1990. Physiological properties of the dorsal longitudinal flight muscle and the tergal depressor of the trochanter muscle of *Drosophila* melanogaster. *J. Muscle Res. Cell Motil.* 11:203–215.
28. Card, G., and M. Dickinson. 2008. Performance trade-offs in the flight initiation of *Drosophila*. *J. Exp. Biol.* 211:341–353.
29. Zumstein, N., O. Forman, …, C. J. Elliott. 2004. Distance and force production during jumping in wild-type and mutant *Drosophila* melanogaster. *J. Exp. Biol.* 207:3515–3522.
30. Collier, V. L., W. A. Kronert, …, S. I. Bernstein. 1990. Alternative myosin hinge regions are utilized in a tissue-specific fashion that correlates with muscle contraction speed. *Genes Dev.* 4:885–895.

31. Wells, L., K. A. Edwards, and S. I. Bernstein. 1996. Myosin heavy chain isoforms regulate muscle function but not myofibril assembly. *EMBO J.* 15:4454–4459.

32. Cripps, R. M., K. D. Becker, …, S. I. Bernstein. 1994. Transformation of *Drosophila* melanogaster with the wild-type myosin heavy-chain gene: rescue of mutant phenotypes and analysis of defects caused by overexpression. *J. Cell Biol.* 126:689–699.

33. Palmer, B. M., Y. Wang, …, D. W. Maughan. 2008. Myofilament mechanical performance is enhanced by R403Q myosin in mouse myocardium independent of sex. *Am. J. Physiol. Heart Circ. Physiol.* 294:H1939–H1947.

34. Larsson, L., and R. L. Moss. 1993. Maximum velocity of shortening in relation to myosin isoform composition in single fibers from human skeletal muscles. *J. Physiol.* 472:595–614.

35. Julian, F. J., L. C. Rome, …, S. Striz. 1986. The maximum speed of shortening in living and skinned frog muscle fibers. *J. Physiol.* 370:181–199.

36. Swank, D. M., G. Zhang, and L. C. Rome. 1997. Contraction kinetics of red muscle in scup: mechanism for variation in relaxation rate along the length of the fish. *J. Exp. Biol.* 200:1297–1307.

37. Lutz, G. J., and L. C. Rome. 1994. Built for jumping: the design of the frog muscular system. *Science.* 263:370–372.

38. Pellegrino, M. A., M. Canepari, …, R. Bottinelli. 2003. Orthologous myosin isoforms and scaling of shortening velocity with body size in mouse, rat, rabbit and human muscles. *J. Physiol.* 546:677–689.

39. Rome, L. C. 1992. Scaling of muscle fibers and locomotion. *J. Exp. Biol.* 168:243–252.

40. Rome, L. C., and S. L. Lindstedt. 1998. The quest for speed: muscles built for high-frequency contractions. *News Physiol. Sci.* 13:261–268.

41. Rome, L. C., C. Cook, …, Y. E. Goldman. 1999. Trading force for speed: why superfast crossbridge kinetics leads to superlow forces. *Proc. Natl. Acad. Sci. USA.* 96:5826–5831.

42. Julian, F. J., L. C. Rome, …, S. Striz. 1986. The influence of free calcium on the maximum speed of shortening in skinned frog muscle fibers. *J. Physiol.* 380:257–273.

43. Trimarchi, J. R., and A. M. Schneiderman. 1995. Flight initiations in *Drosophila* melanogaster are mediated by several distinct motor patterns. *J. Comp. Physiol. [A].* 176:355–364.

44. Bennet-Clark, H. C. 1975. The energetics of the jump of the locust *Schistocerca gregaria*. *J. Exp. Biol.* 63:53–83.

45. Widrick, J. J., J. G. Romatowski, …, R. H. Fitts. 1997. Contractile properties of rat, rhesus monkey, and human type I muscle fibers. *Am. J. Physiol.* 272:R34–R42.

46. Stienen, G. J., J. L. Kiers, …, C. Reggiani. 1996. Myofibrillar ATPase activity in skinned human skeletal muscle fibers: fibre type and temperature dependence. *J. Physiol.* 493:299–307.

47. Lutz, G. J., S. R. Sirsi, …, R. L. Lieber. 2002. Influence of myosin isoforms on contractile properties of intact muscle fibers from *Rana pipiens*. *Am. J. Physiol. Cell Physiol.* 282:C835–C844.

48. Suggs, J. A., A. Cammarato, …, S. I. Bernstein. 2007. Alternative S2 hinge regions of the myosin rod differentially affect muscle function, myofibril dimensions and myosin tail length. *J. Mol. Biol.* 367: 1312–1329.

49. Miller, M. S., C. M. Dambacher, …, D. W. Maughan. 2009. Alternative S2 hinge regions of the myosin rod affect myofibrillar structure and myosin kinetics. *Biophys. J.* 96:4132–4143.

50. Swank, D. M., M. L. Bartoo, …, J. C. Sparrow. 2001. Alternative exon-encoded regions of *Drosophila* myosin heavy chain modulate ATPase rates and actin sliding velocity. *J. Biol. Chem.* 276:15117–15124.

51. Liu, J., M. C. Reedy, …, K. A. Taylor. 2004. Electron tomography of fast frozen, stretched rigor fibers reveals elastic distortions in the myosin crossbridges. *J. Struct. Biol.* 147:268–282.

52. Linari, M., M. K. Reedy, …, G. Piazzesi. 2004. Ca-activation and stretch-activation in insect flight muscle. *Biophys. J.* 87:1101–1111.

53. Nyitrai, M., R. Rossi, …, M. A. Geeves. 2006. What limits the velocity of fast-skeletal muscle contraction in mammals? *J. Mol. Biol.* 355: 432–442.